S FINITE ELEMENT MODELING OF 100% OVERLAPPED CHS UNIPLANAR K-JOINTS (INVESTIGATION OF THE FAILURE MODES)

Leary Pakiding
Program Studi Teknik Sipil Fakultas Teknik Sipil dan Perencanaan
Universitas Sains dan Teknologi Jayapura.
Jl. Raya Sentani, Padang Bulan Abepura-Jayapura, Papua
Email : leary_pakiding@yahoo.com

ABSTRACT

A Finite Element Modeling of 100% Overlapped Circular Hollow Section (CHS) Uniplanar K-Joints has been performed in order to investigate the failure modes. Sixteen variations are modelled using Finite Element Package MARC-Mentat. Based on the Finite Element Analysis, the main area which the failure modes occur is in the intersection between the braces. Brace Local Buckling (BLB) is the most common failure modes that appear in this type of joint. However, this failure mode cannot be directly judged as the failure mode of the joint because it is possible that this is only the failure of the member (lap brace). Additionally onset of cracking (C) also one of the failures that appears in each joint. The last failure mode which appears is the Brace Bending (BB) which only experienced by joints with lower 2γ value.

Keywords **:** K-Joint, Failure Mode, Chord, Brace, Finite Element Modelling

1. INTRODUCTION

In the CIDECT [1], the available formulation for completely overlapped CHS K-joint is based on the analysis of the CHS K gap-joint. This formula should be checked and reevaluated before it can be used. It is mainly because of the fact that the behavior of the Ov≥100 K-joint is different from that of K gap-joint. In the overlapped K-joints, the loads mainly transferred through the two braces without passing the chord. Thus punching shear of the chord can be minimized if compared to that of K gap-joint.

In order to gain more information related to the behaviour of completely overlapped K-joints, a finite element analysis is performed to investigate the joint's failure modes. Parameter study for different value of 2γ and τ is used to see the influence of the variation of different thickness of the chord and the braces in the static strength of the joint. Finally, the result is compared to previous work related.

2. FAILURE CRITERIA AND FAILURE MODE

2.1. Failure Criteria

Based on the work of Dexter et al [6], there are four possible criteria which are considered for each joint. The criteria are:

1. Peak load on load-displacement curve of the compression brace
2. Member squash load
   The axial load in the brace or in the chord may reach the member squash load before true joint failure.
3. 20% tensile strain in the outer surface

This failure criterion represents the onset of cracking in the outer surface of the joint. Although FE joint models may continue to carry increased loads beyond the point of first crack, this criterion is included because any load displacement path beyond this point, being obtained from numerical analysis in which cracking and lamellar tearing are not an integral part of the modeling, may potentially be unconservative.

4. Yura's deformation limit for axial brace loading which is formulated as follows: $\frac{60\sigma_y d}{E}$ (Yura et al. 1980)

2.2. Failure Mode

Form of failure modes which are expected as mentioned in Dexter et al [6] are:

1. Brace Bending (BB) which is associated with high shear deformation.
2. Onset of Cracking (C) related to 20% strain criterion. It can be determined by check of the maximum of strains at the element Gauss points.
3. Brace Local Buckling (BLB) that related to peak load criterion or Yura's limit criterion. This failure mode can be checked directly in the deformed shape of the joint model.

The difference between the failure criteria and the failure mode is that the failure criterion gives indication or requirement to what extend a joint is to fail and it can be seen in the failure mode.

3. FINITE ELEMENT MODELING

3.1. Joint Configurations

The joint configuration which is analyzed can be seen in Figure 1. The 16 parameters which are studied are shown in Table 1. The length of the chord and the braces are taken as such that they do not influence the stress behavior of the joint. The steel grade which is used for this joint member is S355 with yield stress f_y = 355 N/mm^2.

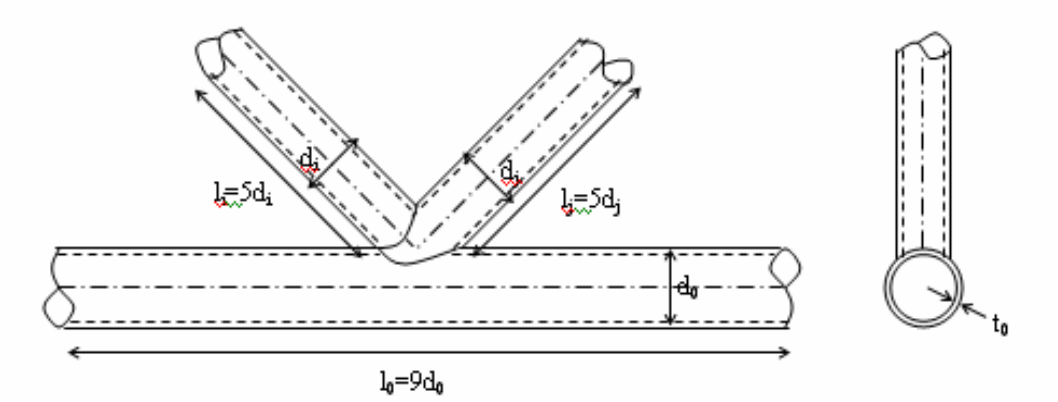

Figure 1. Joint configuration

Table 1. Geometric parameters

Chord		Brace i = Brace j		β	2γ	τ i	θi = θj
do (mm)	to (mm)	di (mm)	ti (mm)	(di/do)	(do/to)	(ti/to)	
200	13.3	120	4.00	0.6	15.0	0.3	45
200	13.3	120	6.65	0.6	15.0	0.5	45
200	13.3	120	7.98	0.6	15.0	0.6	45
200	13.3	120	13.3	0.6	15.0	1.0	45
200	8.0	120	2.40	0.6	25.0	0.3	45
200	8.0	120	4.00	0.6	25.0	0.5	45
200	8.0	120	4.80	0.6	25.0	0.6	45
200	8.0	120	8.00	0.6	25.0	1.0	45
200	5.71	120	1.71	0.6	35.0	0.3	45
200	5.71	120	2.86	0.6	35.0	0.5	45
200	5.71	120	3.43	0.6	35.0	0.6	45
200	5.71	120	5.71	0.6	35.0	1.0	45
200	3.15	120	0.95	0.6	63.5	0.3	45
200	3.15	120	1.58	0.6	63.5	0.5	45
200	3.15	120	1.89	0.6	63.5	0.6	45
200	3.15	120	3.15	0.6	63.5	1.0	45

Remarks : Rows with shading are realistic
Rows without shading are not realistic and meant for parameter study only

3.2. Boundary Conditions

The boundary conditions are shown in Figure 2. For the pinned support, the displacement on y direction and z direction are free and the others DOF are fixed. Additionally, for the rolled support only the displacement on y direction and z direction are set fixed and the others DOF are free. The chord is preloaded in this case.

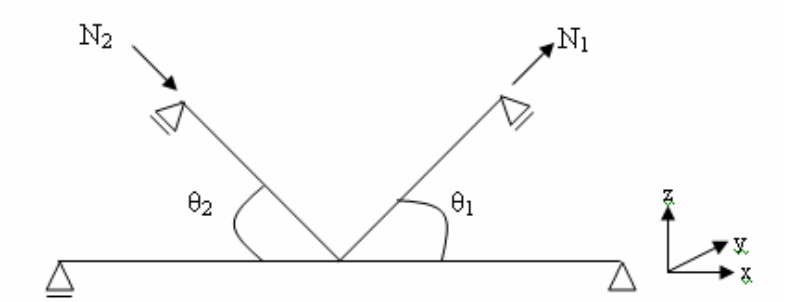

Figure 2. Boundary conditions

These boundary conditions are chosen to simulate what is usually used in the real laboratory experiment work. Additionally, force control is chosen instead of the displacement control.

3.3. Finite Element Analysis

The finite element analysis is done using FE package MARC together with MENTAT for the pre-processing and post-processing. The joints are modeled using four-noded thick shell elements (Marc element type 75) and the properties of this element as described in MARC [2]. The

boundary conditions are applied at the end of the member of the joint using Rigid Body Element type 2 (RBE '2). These boundary conditions are given in order to avoid rigid body movement of the joint. In addition, the welded is not included in the modeling of this joint because of the complexity of the welding to be modeled. The model can be seen in Figure 3.

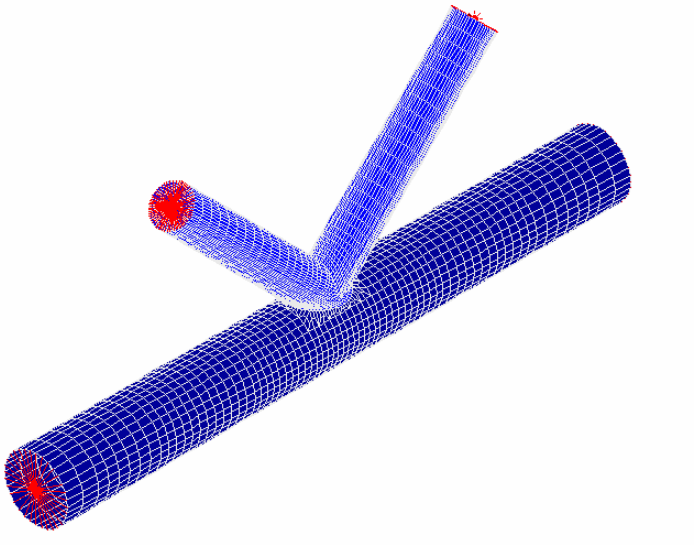

Figure 3. K-Joint model

The true stress-strain curve is used in order to simulate the nonlinear material behavior. This true stress strain curve is based on Van der Vegte [4] and it is shown in Figure 4. For the material properties, Young's modulus is taken based on the true stress strain diagram and the Poisson's ratio is assumed 0.3.

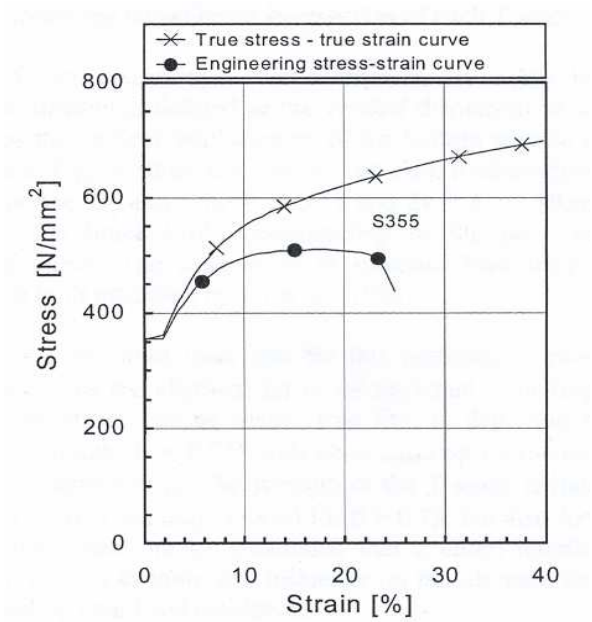

Figure 4. Engineering true stress-strain curve

In the analysis option of the FE program, static analysis is performed where the full Newton-Raphson iterative procedure is activated in the solution control. The criteria for residual forces are used for the convergence test with default value of 10%. For the loading of the joint, the load control is used where the number of loads for both braces was the same as they increased with time.

Moreover, the adaptive time stepping in arc length procedure with default method (modified Riks-Ramm) is used. For this time stepping, all parameters value are taken same to the default of MARC except for the maximum increment which was 300. Finally, large displacement, large strain additive, and updated Lagrange were activated for a complete large strain formulation.

4. RESULTS, VALIDATIONS AND DISCUSSIONS

4.1. Results

The numerical results of the parametric study are presented in Table 2. The capacity of the joint, the failure criteria and the failure modes are given for each joint configuration.

Table 2. Result of geometric parameters study

β (di/do)	2γ (do/to)	τ i (ti/to)	Capacity kN	Failure criteria	Failure modes
0.6	15.0	0.3	251.1	20% ε	C, BLB, BB
0.6	15.0	0.5	476.3	20% ε	C, BLB, BB
0.6	15.0	0.6	592.1	20% ε	C, BLB, BB
0.6	15.0	1.0	1099.7	20% ε	C, BLB, BB
0.6	25.0	0.3	116.1	peak load	BLB
0.6	25.0	0.5	222.1	20% ε	C, BLB
0.6	25.0	0.6	273.9	20% ε	C, BLB
0.6	25.0	1.0	512.3	20% ε	C, BLB
0.6	35.0	0.3	68.5	peak load	BLB
0.6	35.0	0.5	135.2	20% ε	C, BLB
0.6	35.0	0.6	166.1	20% ε	C, BLB
0.6	35.0	1.0	306.1	20% ε	C, BLB
0.6	63.5	0.3	33.2	peak load	BLB
0.6	63.5	0.5	57.3	20% ε	C, BLB
0.6	63.5	0.6	69.9	20% ε	C, BLB
0.6	63.5	1.0	122.9	20% ε	C, BLB

In addition, in Figure 5, the deformed shape (failure mode) for each joint model is presented by the plot of equivalent plastic strain.

The load displacement curves are plotted in Figure 6. The curves are presented in relation to τ and 2γ. The x-axis represents the ratio between the lap brace displacement and its diameter ($\delta 1/d_1$). The y-axis gives the ratio between lap brace axial load and the capacity of the member (lap brace).

As can be seen in Figure 6, there are no joints which reach the full over brace capacity. The maximum capacity which can be achieved is around 70% and the minimum capacity is around 25%.

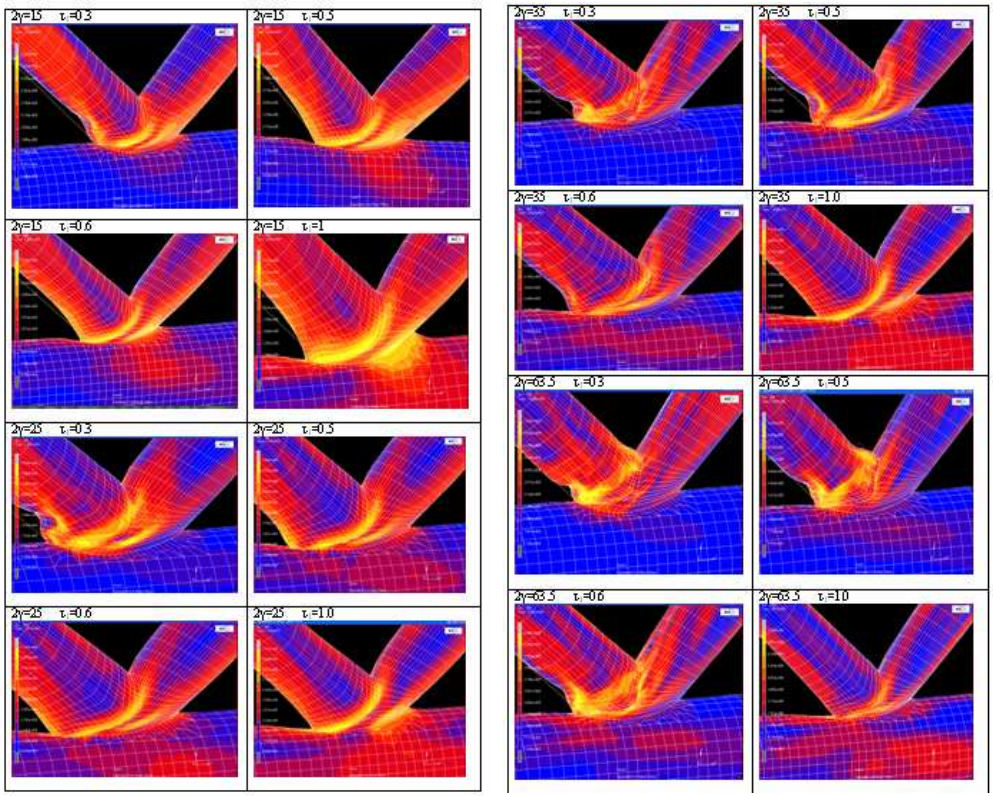

Figure 5. The deformed shape of the joints

4.2. Validations

In order to validate this numerical study, a comparison is made to a related work. The criteria which are used as the comparison tool based on Wardenier [8]. For the Roik interaction criterion, brace shear criterion and brace effective width criterion, the formula which were used to calculate the value are as follows:

Roik Interaction (Local chord yield) criterion

This criterion shows the M-N interaction for local chord plastification due to axial load and bending moment. If the value of M-N interaction exceeds 1.0 it means that failure due to local chord plastification has occurred.

$$\left(\frac{N_0}{N_{pl,0}}\right)^{1.7} + \frac{M_0}{M_{pl,0}} \leq 1.0$$

Where:

$N_0 = 2 * N_1 \cos \theta_1$
$N_{pl,0} = A_0 * fy_0$

$M_0 = 0.5 * 2 * N_1 * e$; $e = 0.5\, d_0$
$M_{pl,0}=(d_0-t_0)^2 * t_0 * f_{y0}$

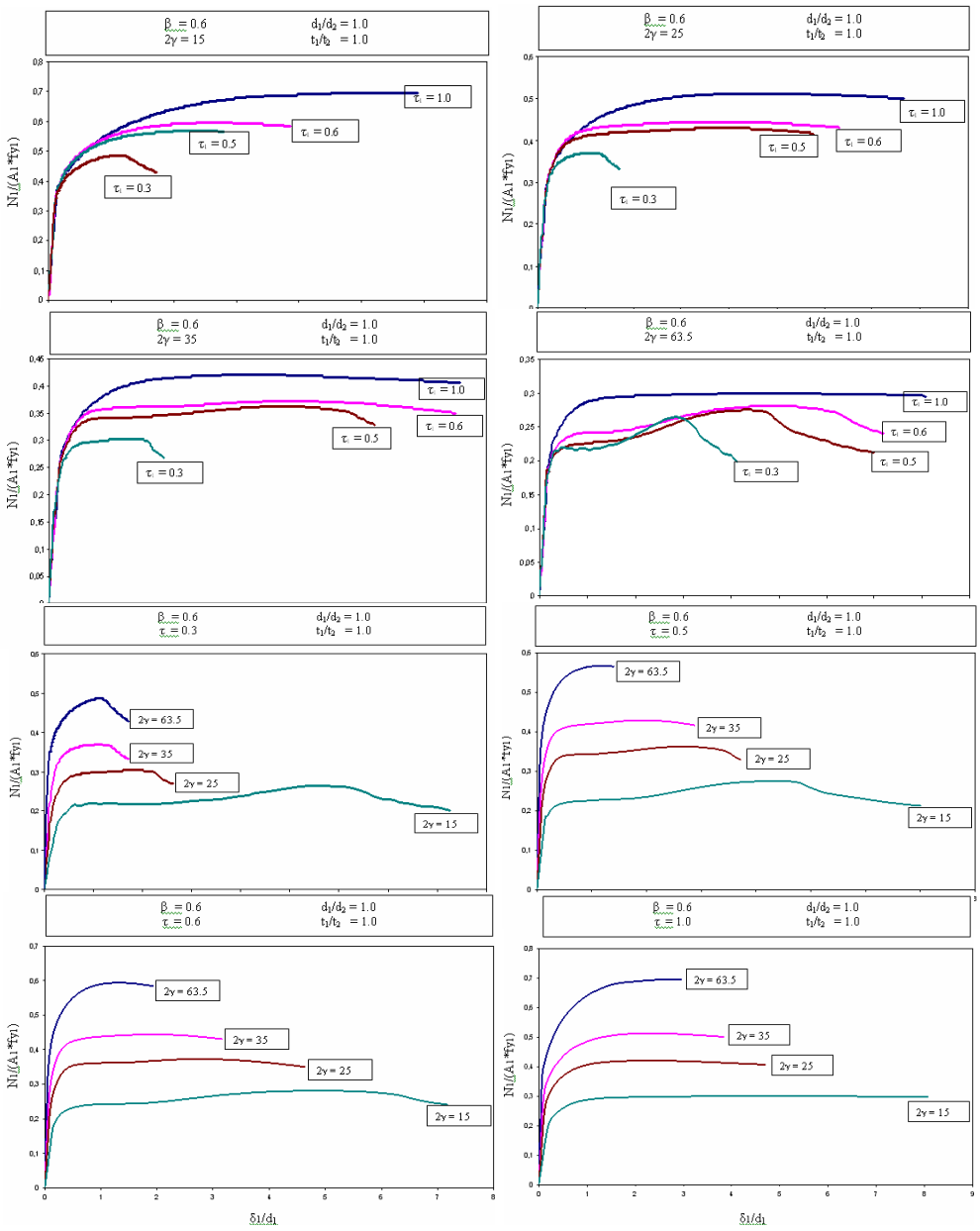

Figure 6. Load-displacement curves

Brace shear

$$N_i \cos\theta_i + N_j \cos\theta_j \le \frac{f_{uj} \cdot t_j}{\sqrt{3}} \cdot \frac{\pi}{4} \frac{\left(3d_j + d_{ej}\right)}{\sin\theta_j}$$

Where:

$$d_{ej} = \left(\frac{12}{d_0 / t_0}\right).\left(\frac{f_{y0}.t_0}{f_{yj}.t_j}\right).d_j \qquad \text{but} \le d_j$$

Brace effective width

$$N_i^* = f_{yi} \cdot t_i \cdot \frac{\pi}{4}\left(3d_i + d_{e,ov} - 4 \cdot t_i\right)$$

Where:

$$d_{e,ov} = \left(\frac{12}{d_j / t_j}\right).\left(\frac{f_{yj}.t_j}{f_{yi}.t_i}\right).d_i \qquad \text{but} \le d_i$$

Figure 7 shows a comparison of the three failure criteria based on the formula given above with the work of Dexter et al [6]. The explanation of this figure is given in the following chapter.

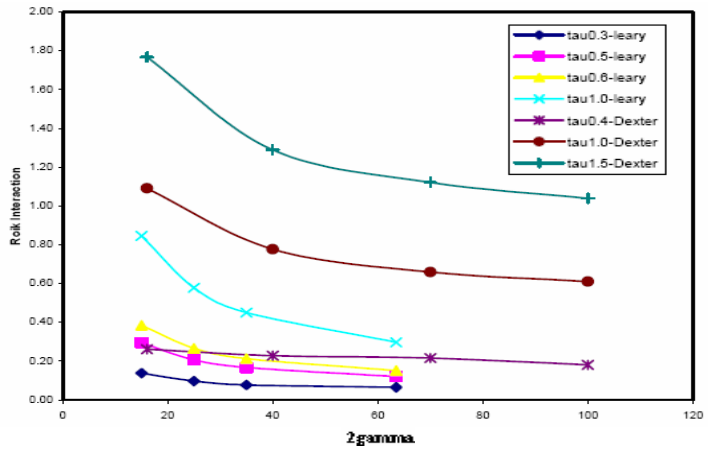

(a)

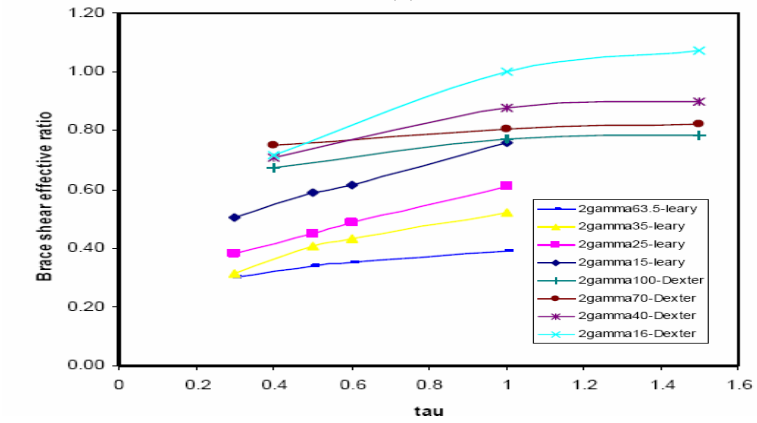

(b)

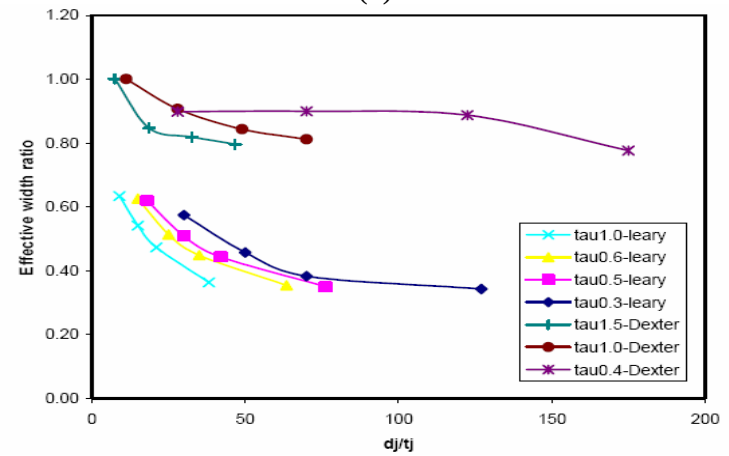

(c)

Figure 7. Comparison of failure criterion to that of Dexter's work.
(a) Roik interaction, (b) brace shear effective ratio, (c) effective width ratio

4.3. Discussions

As shown in Figure 5, failure of 100% overlapped K-joint mostly occurs in both braces. In addition Table 2 shows that an increasing τ_1 value with constant 2γ and β results in an increased capacity of the joint. This can also clearly seen in Fig.6. However, none of the graphs show a condition where the joint reach the full (100%) efficiency. Moreover, Table 2 also shows that for low value of τ_1 with different 2γ value, the result in failure modes are found to be the same for the joints with exception for τ_1=0.3 and 2γ=15.

The majority of the joint reveals that BLB is the most common failure mode and this is also found in the work of Dexter et al [5], Fung et al [8] and Healy [3]. Next to it is the onset of cracking (C) which reveals in the through brace. BB failure mode only appears for 2γ=15.

Comparison of this analysis result to that of Dexter et al [6] (Figure 7) shows that there are considerable differences. This may be the result of the fact that the numerical analysis which is done here have different parameters compare to that of Dexter. Nevertheless, as can be seen in Figure 7, the tendencies of the results have the same pattern. These can be explained as follows:

1. For the Roik interaction criterion, Dexter's works show that with increasing 2γ value the Roik interaction value was reduced and the same condition occurs for the results of this study. In addition, an increasing τ_1 value results in an increase of the Roik interaction value.
2. Related to the brace shear criterion, the same tendency of the curves is found for the Dexter results and of this study. In this case, an increasing τ_1 and 2γ results in an increased value of brace shear.
3. Finally for the effective width criterion the same pattern occurs for both works.

5. CONCLUSIONS

Based on the result of finite element analysis it is found that the location of the failure in the 100% overlapped K-joints mainly occur in the intersection between the braces. BLB is the dominant failure modes. However, this type of failure cannot be guaranteed as the failure mode of the joint. A careful checked should be performed by assuring that the failure is not the member's failure (lap brace failure). Another type of failure which also govern the joint is the onset of cracking which corresponds to 20% tensile strain in the outer surface. Finally Brace Bending is the failure mode which arise and experienced by joints with lower 2γ value.

NOTATION

BLB = Brace Local Buckling
C = Onset of Cracking
BB = Brace Bending
N_0 = Axial force of the chord
$N_{0,pl}$ = Plastic axial force of the chord
M_0 = Moment of the chord
$M_{0,pl}$ = Plastic moment of the chord
N_1 = Axial force of lap brace
d_0 = chord diameter
d_i,d_j = brace diameter
t_0 = chord thickness
t_i,t_j = brace thickness
f_y = yield stress
β = diameter ratio (d_i/d_0)
2γ = chord radius to thickness ratio (d_0/t_0)
τ = wall thickness ratio (t_i/t_0)
θ = brace angle

REFERENCES

Dexter E.M, Lee M.M.K, Kirkwood M.G., 1996, *Overlap K joints in circular hollow sections under axial loading*, 118, J Offshore Mech Arctic Engng OMAE, 53–61.

Dexter E.M, Lee M.M.K., 1998, *Effect of overlap on the behaviour of axially loaded K-joints*, 8th International Symposium on Tubular Structures, Singapore, pp 249-58.

Fung T.C, Soh C.K, Gho W.M., 2001, *Ultimate capacity of completely overlapped tubular joints II: Behavioral study*, J Construct Steel Res, 57(8):881-06.

Healy B.E., 1994, *A numerical investigation into the capacity of overlapped circular K-Joints*, 6th International Symposium on Tubular Structures, Melbourne, Australia, pp 563-71.

MARC user's manual and primer., 1993, MARC Analysis and Research Corporation, Palo Alto (CA).

Van der Vegte G.J., 1995, *The static strength of uniplanar and multiplanar tubular T- and X- joints*, Delft University Press, The Netherlands.

Wardenier J, et al., 1991, *Design Guide for Circular Hollow Section (CHS) Joints under Predominantly Static Loading*, CIDECT.

Wardenier J, 2006, IIW Doc. XV-E-06-319.